Identification of Motile Sperm Domain–Containing Protein 2 as Regulator of Human Monocyte Migration

Itzhak Mendel, Niva Yacov, Yaniv Salem, Oshrat Propheta-Meiran, Eti Ishai, and Eyal Breitbart

Binding of chemokines to their cognate receptors on monocytes instigates a cascade of events that directs these cells to migrate to sites of inflammation and cancerous tissues. Although targeting of selected chemokine receptors on monocytes exhibited preclinical efficacy, attempts to translate these studies to the clinic have failed thus far, possibly due to redundancy of the target receptor. We reveal that motile sperm domain–containing protein 2 (MOSPD2), a protein with a previously unknown function, regulates monocyte migration in vitro. This protein was found to be expressed on the cytoplasmic membrane of human monocytes. Silencing or neutralizing MOSPD2 in monocytes restricted their migration when induced by different chemokines. Mechanistically, silencing MOSPD2 inhibited signaling events following chemokine receptor ligation. When tested for expression in other immune cell subsets, MOSPD2 was apparent also, though less abundantly, in neutrophils, but not in lymphocytes. Thus, in the presence of neutralizing Abs, neutrophil migration was inhibited to some extent whereas lymphocyte migration remained intact. In view of these results, we suggest MOSPD2 as a potential target protein for treating diseases in which monocyte and neutrophil accumulation is correlated with pathogenesis. *The Journal of Immunology*, **2017, 198: 2125–2132.**

Chemokines and their cognate receptors play an important role in regulating the migration of leukocytes (1). Chemokine-induced arrival of monocytes into assaulted tissues is imperative for the resolution of inflammation. Nonetheless, studies have shown that monocytes are also mediators of inflammatory diseases and tumor development. In atherosclerosis, monocytes migrate into the atherosclerotic plaque to induce the production of proinflammatory cytokines and promote plaque venerability and rupture (2). CCR2/ApoE or CCR5/ApoE double-deficient mice demonstrated reduced lesion size and fewer infiltrating monocytes in the aorta (3, 4). In an experimental autoimmune encephalomyelitis model of multiple sclerosis, infiltrating monocytes accounted for the initiation of demyelination (5), and in rheumatoid arthritis, in which a vast population of pannus infiltrating cells consists of monocytes/macrophages, targeting chemokine receptors abundantly expressed by these cells reduced synovial inflammation (6). Recent accumulating evidence indicates that tumor-associated macrophages that originate from infiltrating circulating monocytes promote tumor progression (7–9). In a mouse model of breast cancer, recruitment of CCL2-mediated monocytes facilitated tumor metastasis (7). Secretion of periostin by glioblastoma cells recruited tumor-associated macrophages that enhanced tumor growth (10), whereas removal of circulating and intratumor macrophages in melanoma-bearing mice inhibited tumor growth (11). Taken together, these studies suggest that limiting monocyte migration may improve clinical outcome in inflammatory diseases and cancer. However, human studies targeting specific chemokine ligands or receptors in inflammation and cancer have failed thus far to produce positive results.

We previously showed that VB-201, an oxidized phospholipid small molecule of the lecinoxoid family, inhibits signaling downstream to chemokine receptors and migration thereof in human monocytes, regardless of the activating chemokine (12). In the current study, comparative analysis by mass spectroscopy using biotin labeled VB-201 (BIO-VB-201) and another member of the lecinoxoid family, VB-221 (BIO-VB-221), which does not affect monocyte migration, revealed a protein to which no function has previously been ascribed. This protein was named motile sperm domain–containing protein 2 (MOSPD2). We show that MOSPD2 expression is localized to the plasma membrane in $CD14^+$ human monocytes, and is also apparent in neutrophils, but not in lymphocytes. Most importantly, we discovered, using gene silencing and mAbs, that MOSPD2 promotes migration of these myeloid cells in vitro.

Materials and Methods

Human immune cell subsets

Venous blood samples were obtained from healthy male donors in compliance with the Institutional Review Board at Sheba Medical Center, Ramat Gan, Israel. PBMCs were isolated on Ficoll-Paque PLUS (GE Healthcare) using 50 ml Leucosep tubes (Greiner Bio-One). Cells were washed in PBS (Biological Industries, Beit Haemek, Israel), and incubated at 4°C for 15 min in buffer containing PBS and 0.5% BSA with human CD14, *Pan* T cell, and CD19 microbeads. Neutrophils were separated from whole blood using CD66abce microbeads (Miltenyi Biotec, Bergisch Gladbach, Germany). To generate macrophages, $CD14^+$ monocytes were differentiated with GM-CSF (100 ng/ml) or M-CSF (100 ng/ml) for 7–10 d.

Synthesis and biotin labeling of VB-201 and VB-221

Synthesis and biotin labeling of VB-201 was performed as described previously (13). VB-221 was synthesized and labeled in a similar manner, except for the starting compound of the latter (methanesulfonic acid-2-octyl-dodecyl ester).

VBL Therapeutics, Or Yehuda 6037604, Israel

Received for publication September 27, 2016. Accepted for publication December 28, 2016.

Address correspondence and reprint requests to Dr. Itzhak Mendel, VBL Therapeutics, 6 Yehonatan Netanyahu Street, Or Yehuda 6037604, Israel. E-mail address: Itzhak@vblrx.com

The online version of this article contains supplemental material.

Abbreviations used in this article: CRAL, cellular retinaldehyde binding protein; HA, hemagglutinin; MOSPD2, motile sperm domain–containing protein 2; MudPIT, Multidimensional Protein Identification Technology; sh, short hairpin.

www.jimmunol.org/cgi/doi/10.4049/jimmunol.1601662

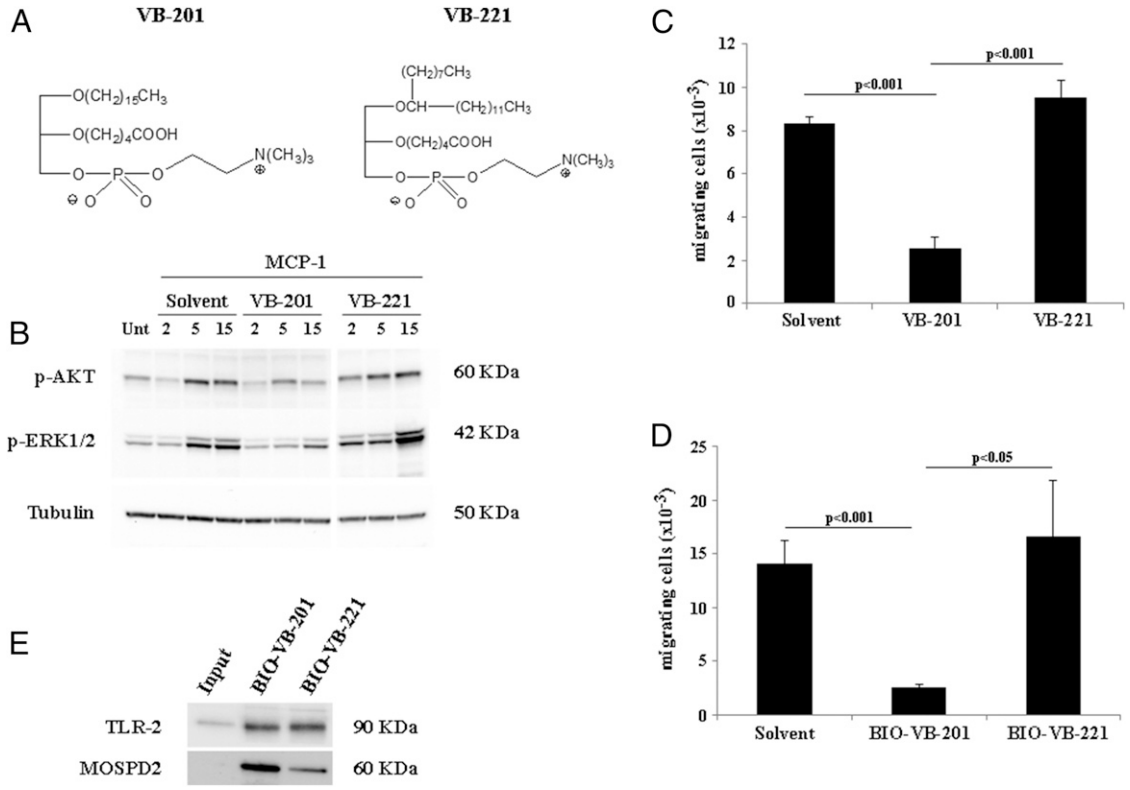

FIGURE 1. MOSPD2 is a potential regulator of monocyte migration. (**A**) Chemical structure of VB-201 and VB-221. (**B** and **C**) MCP-1–induced signaling (one of three experiments) and migration of $CD14^+$ monocytes (sum of three experiments) in the presence of 7.5 μM of VB-201 or VB-221, as described in *Materials and Methods*. Cell count is presented. (**D**) MCP-1–induced migration of monocytes in the presence of BIO-VB-201 or BIO-VB-221, as described in *Materials and Methods*. Sum of two experiments is shown. Cell count is presented. (**E**) Precipitation of proteins from $CD14^+$ monocytes with BIO-VB-201 or BIO-VB-221. Immunoblotting was performed with anti–TLR-2 or anti-MOSPD2. Three independent experiments were performed.

Subcellular fractionation

Cellular compartments were fractionated using the Subcellular Protein Fractionation Kit (Thermo Fisher Scientific) according to the manufacturer's instructions.

Table I. Comparative mass spectrometry results for MOSPD2 from primary human monocyte cell lysates precipitated with BIO-VB-201 or BIO-VB-221

Protein (Accession Number): MOSPD2 (Q8NHP6)		
	Mascot score for individual peptides	
Unique Peptide Sequences	BIO-VB-201	BIO-VB-221
LQQDDNWVESYLSWR	79	n.d.
EISVNDLNESSIPR	71	19
TLIVLTNVTK	64	n.d.
HNIVDETLK	57	36
IVIFDMPWLMNAAFK	50	n.d.
LIAFWLER	47	n.d.
GPLLHISPAEELYFGSTESGEKK	38	n.d.
TWLGPEAVSLLK	37	n.d
FIINCFK	27	n.d.
INPTESTSKAEENEKVDSK	13	n.d.
MLDESFQWRK	15	n.d.
RFEAEYVTDK	31	n.d
KLEDQVQR	13	n.d
Overall Mascot score	619	36

The table shows all of the identified MOSPD2 peptide sequences with their respective scores as well as the overall score using the Mascot search engine. One of two experiments is shown.

n.d., not detected.

MOSPD2 silencing

The U937 monocytic cell line was purchased from American Type Culture Collection (CRL-1593.2). The cells (2×10^6 in 2 ml) were placed in a 15 ml tube. Lentiviral particles expressing control short hairpin (sh) RNA (2×10^5 viral particles) (SHC202V, 5′-CCGGCAACAAGATGAAGAGCACCAACTCGAGTTGGTGCTCTTCATCTTGTTGTTTTT-3′; Sigma) or human MOSPD2 sh-RNA (2×10^6 viral particles) (TRCN0000323142 5′-CCGGCCCAGATGGTTATTGGAAATTCTCGAGAATTTCCAATAACCATCTGGGTTTTTG-3′, MOSPD2 #1; TRCN0000149096-5′-CCGGGCCATACTGTTGAAAGCAGTACTCGAGTACTGCTTTCAACAGTATGGCTTTTTTG-3′, MOSPD2 #2; Sigma) were applied on the cells, which were then spun for 60 min, 2000 rpm at room temperature in the presence of 8 μg/ml polybrene (Sigma). The cells were then seeded in a six-well plate. After 72 h, fresh medium containing 4 μg/ml puromycin (Sigma) was added for the selection of transduced cells.

Generation and isolation of recombinant human MOSPD2 and polyclonal and monoclonal anti-MOSPD2 Ab

For the production of tagged recombinant MOSPD2, full-length human MOSPD2 cDNA was inserted into the lentivirus plasmid vector pLVX-EF1α-IRES-Puro (Clontech). Oligonucleotide encoding the hemagglutinin (HA) tag was inserted upstream to the MOSPD2 coding region. A2058 melanoma line cells (American Type Culture Collection) were transduced with HA-MOSPD2–expressing lentiviral particles (Genecopea, Rockville, MD). For the production of polyclonal Abs, rabbits were immunized with ~0.5 mg HA–recombinant human MOSPD2 emulsified in CFA, followed by three boosts every 3 wk of ~0.25 mg HA–recombinant human MOSPD2 emulsified in IFA. Serum was collected 1 wk after each boost for immunogenicity assessments and titers. Anti-MOSPD2 Abs were isolated from serum using protein A/G beads (Santa Cruz Biotechnology, Santa Cruz, CA). Human mAb against the extracellular region of human MOSPD2 was generated using the HuCAL PLATINUM Platform (Bio-Rad). Briefly, The HuCAL library, which comprises human Abs in a Fab format presented on phage particles, was incubated with immobilized

1 MAENHAQNKAKLISETRRRFEAEYVTDKSDKYDARDVERLQQDDNWVESY 40
LSWRHNIVDETLKMLDESFQWRKEISVNDLNESSIPRWLLEIGVIYLHGYDKE 100
GNKLFWIRVKYHVKDQKTILDKKKLIAFWLERYAKRENGKPVTVMFDLSET 140
GINSIDMDFVRFIINCFKVVYPKYLSKIVIFDMPWLMNAAFKIVKTWLGPEAV 200
SLLKFTSKNEVQDYVSVEYLPPHMGGTDPFKYSYPPLVDDDFQTPLCENGPIT 240
SEDETSSKEDIESDGKETLETISNEEQTPLLKKINPTESTSKAEENEKVDSKVKA 300
FKKPLSVFKGPLLHISPAEELYFGSTESGEKKTLIVLTNVTKNIVAFKVRTTAP 340
EKYRVKPSNSSCDPGASVDIVVSPHGGLTVSAQDRFLIMAAEMEQSSGTGPA 380
ELTQFWKEVPRNKVMEHRLRCHTVESSKPNTLTLKDNAFNMSDKTSEDICLQ 420
LSRLLESNRKLEDQVQRCIWFQQ**LLLSLTMLLLAFVTSFFYLLY**S 480 500

FIGURE 2. Amino acid sequence of human MOSPD2. Bold text is the transmembrane region; underlined text is the CRAL-TRIO domain.

protein, encompassing the extracellular region of human MOSPD2. After washing, specific Ab phage were eluted and used to infect *Escherichia. coli* to generate an enriched Ab phage library for three panning rounds. The enriched Ab DNA was isolated and subcloned into an expression vector to generate bivalent F(ab′)2 fragments in *E. coli*. Colonies were then lysed to release the Ab, and cultures were screened for specific Ag binding by ELISA. Subsequently, unique Abs were expressed, purified using one-step affinity chromatography and tested for specificity by ELISA and by flow cytometry on cells over-expressing human MOSPD2. Flow cytometry positive clones were converted into full IgG1 mAbs by transfecting HKB11 cells with an expression vector that adds the Fc region.

In vitro cell migration

To test for chemotaxis, RANTES (CCL5, 100 ng/ml), MCP-1 (CCL2, 100 ng/ml), MCP-3 (CCL7, 100 ng/ml), MIP-3β (100 ng/ml), or SDF-1 (CXCL12, 25 ng/ml) (PeproTech) were dissolved in 0.5% FBS/RPMI 1640 and placed in the lower chamber of a QCM 24-well migration assay plate (5 μm pores) (Corning-Costar, Corning, NY). Cells (3×10^5) were seeded in the upper chamber, followed by incubation for 3 h, after which the number of cells that migrated to the lower compartment was determined by FACS. Results are shown as mean ± SD.

Western blotting

U937 cells (10^6) transduced with sh-Control or sh-MOSPD2 lentiviral particles were starved for 3 h in 0.5% FCS medium and then activated with RANTES (100 ng/ml, 5 min), MIP-1α (100 ng/ml, 5 min), MCP-3 (100 ng/ml, 5 min), SDF-1 (25 ng/ml, 5 min), IFN-γ (50 ng/ml, 30 min), or PMA (20 ng/ml, 15 min). $CD14^+$ monocytes were starved as above and activated with MCP-1 (100 ng/ml) in the presence of VB-201 or VB-221. The following Abs were used for immunoblotting:

Primary Abs. Tubulin (1:4000) and phospho-extracellular–regulated kinase (p-ERK1/2) (Thr^{183} and Tyr^{185}, 1:4000) from Sigma; total ERK (1:1000), phospho-AKT (Ser^{473}, 1:1000), and p-Stat1 (Tyr^{701}, 1:1000) from Cell Signaling; TLR-2 (1:500) from R&D Systems (Minneapolis, MN); HLA Class 1 ABC (1:1000) from Abcam; heat shock protein (HSP) 90 (1:1000) from Santa Cruz Biotechnology (Dallas, TX); and MOSPD2 polyclonal rabbit Ab (in-house) (1:5000).

Secondary Abs. HRP donkey anti-rabbit (1:5000) and HRP goat anti-mouse (1:5000) from Jackson ImmunoResearch (West Grove, PA).

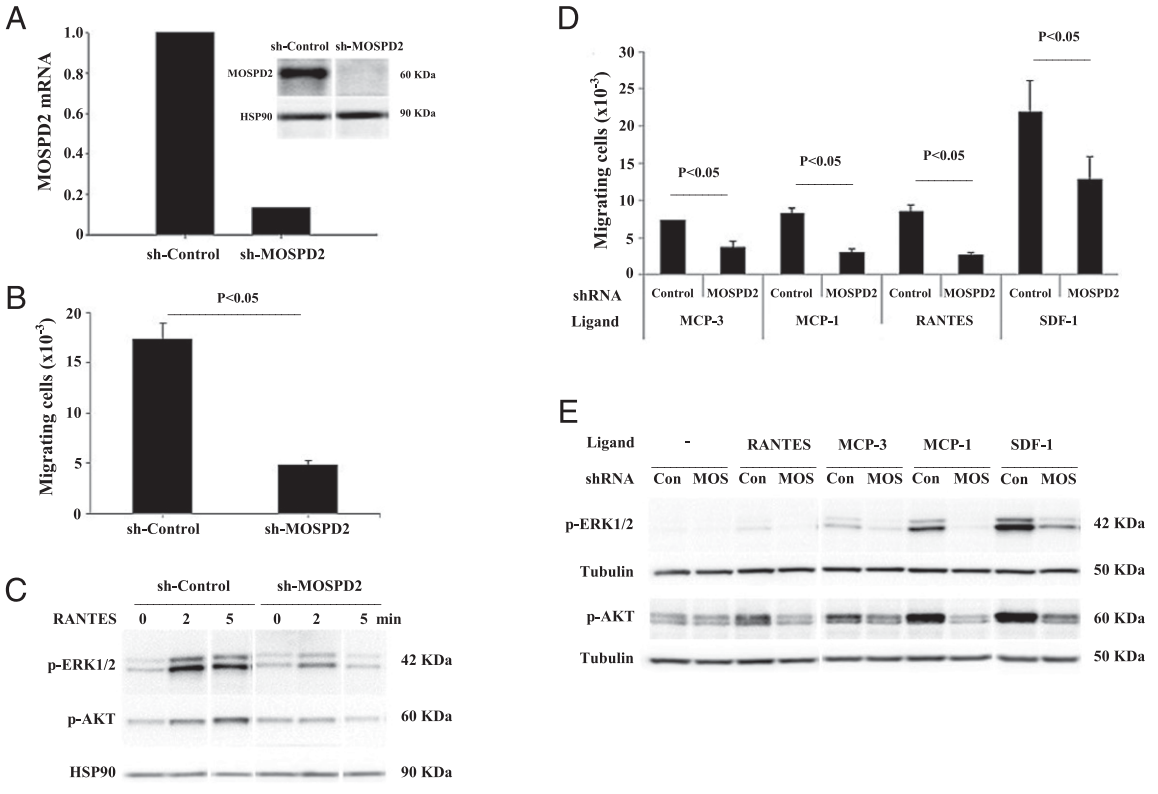

FIGURE 3. MOSPD2 promotes monocytic line migration. (**A**) mRNA and protein expression of MOSPD2 in U937 cells transduced with sh-Control or sh-MOSPD2 #1 lentiviral particles. 18S was used to normalize RNA levels. Samples were run in triplicate. One of at least three experiments is shown. (**B**) Transwell migration of U937 cells transduced with sh-Control or sh-MOSPD2 #1 lentiviral particles toward RANTES (100 ng/ml). Cell count is presented. Samples were run in triplicate. One of four experiments is shown. (**C**) U937 cells transduced with sh-Control or sh-MOSPD2 #1 lentiviral particles were incubated for the indicated time (minutes) with RANTES, and phosphorylation of ERK1/2 and AKT was evaluated. HSP90 was used as loading control. One of three experiments is shown. (**D**) Transwell migration of U937 cells transduced with sh-Control or sh-MOSPD2 #1 lentiviral particles toward MCP-3 (100 ng/ml), MCP-1 (100 ng/ml), RANTES (100 ng/ml), and SDF-1 (25 ng/ml). Cell count is presented. Samples were run in triplicate. One of three experiments is shown. (**E**) U937 cells transduced with sh-Control or sh-MOSPD2 #1 lentiviral particles were incubated for 5 min with MCP-3 (100 ng/ml), MCP-1 (100 ng/ml), RANTES (100 ng/ml), and SDF-1 (25 ng/ml), and phosphorylation of ERK1/2 and AKT was evaluated. Tubulin was used as loading control. One of three experiments is shown.

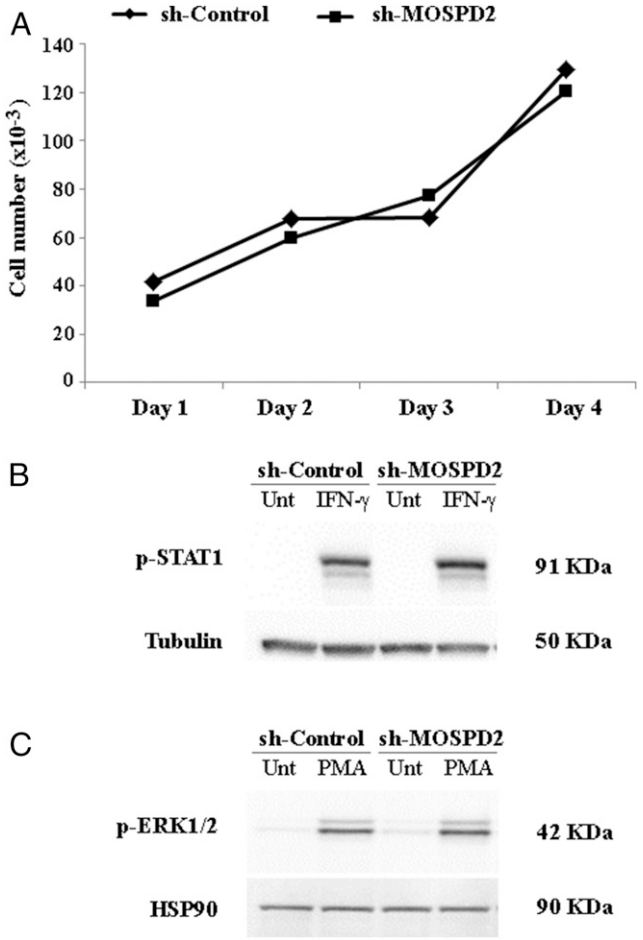

FIGURE 4. MOSPD2 does not affect proliferation, IFN-γ–induced activation, or protein kinase C–mediated activation. (**A**) Proliferation of U937 cells transduced with sh-Control or sh-MOSPD2 #1 lentiviral particles. One of at least three experiments is shown. (**B**) U937 cells transduced with sh-Control or sh-MOSPD2 #1 lentiviral particles were activated with IFN-γ for 30 min (50 ng/ml), and phosphorylation of Stat1 was evaluated. Tubulin was used as loading control. One of three experiments is shown. (**C**) U937 cells transduced with sh-Control or sh-MOSPD2 #1 lentiviral particles were incubated with PMA for 15 min (20 ng/ml), and phosphorylation of ERK1/2 was evaluated. HSP90 was used as loading control. One of three experiments is shown.

MOSPD2 transfection

HEK 293 cells were transfected for 48 h with empty plasmid or plasmid encoding HA-tagged human MOSPD2 using jetPRIME transfection reagent (Polyplus-transfection). Transfection efficiency was determined by flow cytometry gating on live cells and using anti–HA-PE Ab (Miltenyi Biotec).

Precipitation

Cells were lysed using a 1% NP-40 lysis buffer containing 1:100 protease and phosphatase inhibitors, followed by 20 min incubation on ice and 15 min centrifugation at maximum speed. Samples were incubated in a rotator overnight at 4°C with BIO-VB-201 or BIO-VB-221. Streptavidin agarose beads (Sigma) were added for 2 h. Protein elution was performed with loading buffer containing 62.5 mM Tris, 2.3% SDS, and 10% glycerol and 0.02% pyronin for 10 min at room temperature.

Mass spectrometry protein identification and results validation

Following precipitation, samples were resolved on SDS-PAGE gel and visualized using Imperial Protein Stain (Thermo Scientific). Whole lanes corresponding to BIO-VB-201 and BIO-VB-221 treated cells were cut into five pieces each. The samples were digested with trypsin and analyzed by LC-MS/MS on an LTQ-Orbitrap mass spectrometer (Thermo Scientific). Proteins were identified using Discoverer software version 1.3 against the human part of the SWISS-PROT database using the Mascot search engine. For Mascot results, the score is determined by: 1) standard score, which is the cumulative protein score based on summing the ion scores of the unique peptides identified for that protein. If a peptide is redundantly identified, only the highest scoring peptide is used; or 2) Multidimensional Protein Identification Technology (MudPIT) score, which is the sum of the ion excess score over the homology or identity threshold for each spectrum plus the average threshold. For MudPIT scoring, the score for each peptide is not its absolute score but rather the amount by which it exceeds the threshold. Therefore, peptides with a score below the threshold do not contribute to the score. For each peptide, the threshold is the homology threshold, if it exists; otherwise, it is the identity threshold. By default, the Proteome Discoverer application automatically alternates between the standard score and the MudPIT score to calculate the protein score in the Mascot node results. The Proteome Discoverer application automatically uses the MudPIT score when the number of queries divided by the number of entries in the FASTA protein database exceeds 0.001.

For result validation, cells were lysed and precipitated with BIO-VB-201 or BIO-VB-221 as described above. Lysates were resolved on SDS-PAGE gel and transferred to nitrocellulose membrane. TLR-2 (1:500) from R&D Systems and MOSPD2 polyclonal rabbit Ab (in-house) (1:5000) were used for immunoblotting followed by incubation with HRP donkey anti-rabbit (1:5000).

Quantitative PCR

To determine MOSPD2 mRNA expression level, RNA was extracted from cells using RNeasy Mini Kit (Qiagen, Valencia, CA). For cDNA preparation, 2 μg of RNA was combined with qScript Reaction Mix and qScript Reverse Transcriptase (Quanta Bioscience, Gaithersburg, MD). Real-time PCR reactions were performed using sets of primers for human MOSPD2 (Forward 5′-TGTGACCCGGGTGCATC-3′ Reverse 5′-TCCATTTCTG-CAGCCATTATCA-3′) and 18S (Forward 5′-GACTCTTTCGAGGCCCT-GTAATT-3′ Reverse 5′-ACCAGACTTGCCCTCCAATG-3′) to normalize RNA levels (Biosearch Technologies, Petaluma, CA) and SYBR Green PCR Master Mix (Applied Biosystems, Warrington, U.K.).

Cell proliferation

U937 cells transduced with sh-Control or sh-MOSPD2 lentiviral particles were seeded in six-well plates (10^4 per well). The cells were counted in triplicate by FACS every 24 h for three consecutive days.

Immunohistochemistry

Formalin-fixed paraffin-embedded tissues were purchased from Proteogenex (Culver City, CA). Anti-CD163 (MRQ-26; Cell Marque, Rocklin, CA) or/and anti-MOSPD2 (HPA003334; Sigma), diluted at 1:80 and 1:100, respectively, were used for staining.

Statistical analysis

Data were analyzed using SigmaPlot 12. The Student *t* test or Mann–Whitney *U* test was used for comparison between two groups.

Results

Initial identification of MOSPD2 as a potential regulator of monocyte migration

VB-201 was previously shown to perturb chemokine-induced migration and signaling events in human $CD14^+$ monocytes; however, the target Ag through which VB-201 mediates its inhibitory effect on monocyte migration is unknown. VB-201 and its derivative molecule VB-221 (Fig. 1A) inhibit TLR-2– and TLR-4–induced activation (13) (Y. Salem, N. Yacov, E. Ishai, I. Mendel, E. Breitbart, unpublished observations); yet VB-221, unlike VB-201, does not impair chemokine-induced migration and downstream signaling (Fig. 1B, 1C). We labeled VB-201 and VB-221 with biotin, applied them separately to cell lysates of $CD14^+$ monocytes, and used mass spectroscopy to search for proteins that precipitate differentially. Fig. 1D shows that BIO-VB-201 and BIO-VB-221 did not alter their differential effect on monocyte migration. Mass spectroscopy analysis revealed that MOSPD2, a protein with no hitherto assigned functionality, precipitated differentially with BIO-VB-201 and BIO-VB-221 (Table I). Based on UniProtKB, the 518 aa long human MOSPD2 contains a

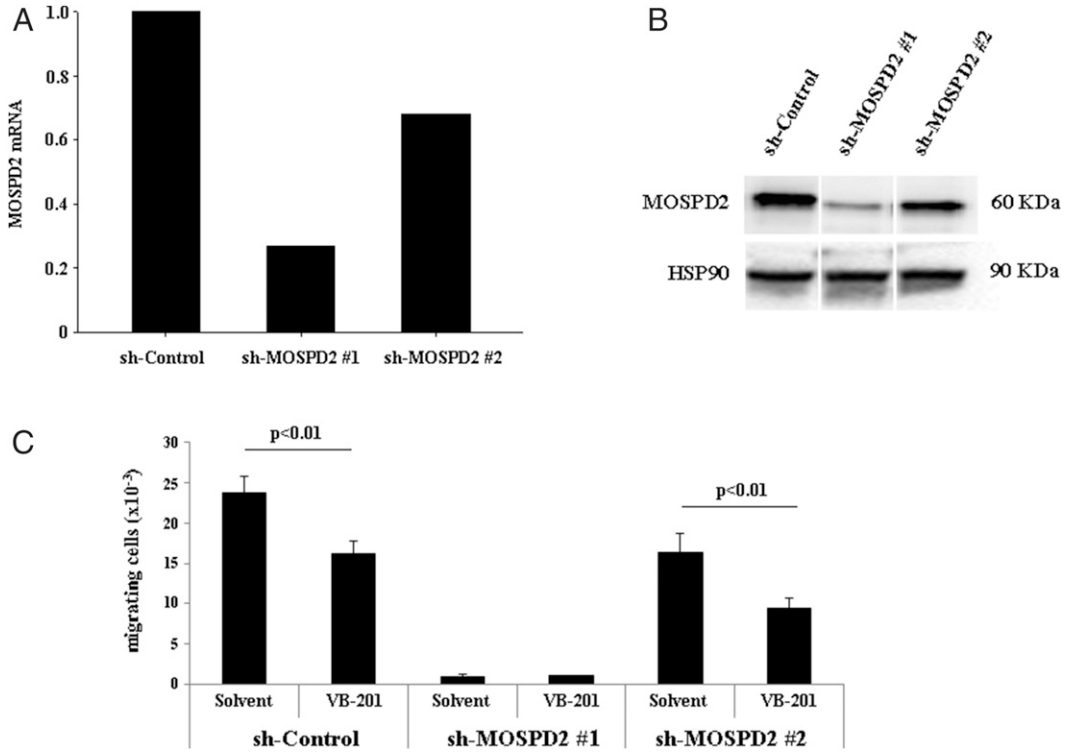

FIGURE 5. Effect of VB-201 on migration of MOSPD2-silenced monocytes. (**A**) MOSPD2 mRNA levels in U937 cells transduced with sh-Control and sh-MOSPD2 lentiviral particles targeting two different regions. 18S was used to normalize RNA levels. Samples were run in triplicate. One of three experiments is shown. (**B**) Precipitation with BIO-VB-201 of MOSPD2 from cells in (A). Immunoblotting was performed with anti-MOSPD2. HSP90 demonstrates the equal number of cells between samples before precipitation. One of two independent experiments is shown. (**C**) Transwell migration of U937 cells transduced with sh-Control or sh-MOSPD2 lentiviral particles targeting two different regions toward SDF-1 (100 ng/ml) was tested with or without 7.5 μM VB-201. Cell count is presented. Samples were run in triplicate. One of three experiments is shown.

cellular retinaldehyde binding protein (CRAL)-TRIO domain and is predicted to have one transmembrane region at position 497–517 (Fig. 2). In order to validate mass spectroscopy results, cell lysates from $CD14^+$ monocytes were precipitated with BIO-VB-201 or BIO-VB-221 and blotted for MOSPD2. Results were in line with our previous findings: BIO-VB-201 and BIO-VB-221 bound similarly to TLR-2, whereas MOSPD2 precipitated only with BIO-VB-201 (Fig. 1E). We therefore hypothesized that MOSPD2 promotes monocyte migration and that VB-201 may inhibit MOSPD2 function.

MOSPD2 promotes chemokine-induced monocytic cell line migration

To establish a role for MOSPD2 in human monocytes, we initially silenced its expression in a monocytic cell line. To that end, U937 monocytic cell line was transduced with sh-Control or sh-MOSPD2 lentiviral particles. Fig. 3A demonstrates the silencing efficacy of sh-MOSPD2 as assessed by quantitative PCR and Western blot. When tested for migration, we found that MOSPD2-silenced cells were severely impaired in their ability to migrate in vitro toward RANTES (CCL5) (Fig. 3B). Two major signaling pathways recognized as crucial for monocyte migration are the MEK–ERK and PI3K–AKT pathways (14, 15). We therefore tested whether silencing MOSPD2 expression perturbs the activation of AKT and/or ERK. The results in Fig. 3C show that phosphorylation of ERK and AKT in the presence of RANTES is completely suppressed in MOSPD2-silenced cells. We then wished to ascertain whether the effect observed is restricted to only one chemokine. To that end, sh-Control– and sh-MOSPD2–silenced U937 cells were activated with ligands that induce migration and phosphorylation via different chemokine receptors. We found that silencing MOSPD2 impaired monocyte migration and ERK and AKT phosphorylation regardless of the chemokine used (Fig. 3D, 3E). This outcome did not result from alterations in the surface expression of the corresponding chemokine receptors (Supplemental Fig. 1). We also examined whether targeting MOSPD2 compromises any biological functions of monocytes other than migration. Proliferation of U937 was comparable between sh-Control– and sh-MOSPD2–transduced cells (Fig. 4A) as was priming with IFN-γ or protein kinase C (Fig. 4B, 4C). These results suggest that MOSPD2 specifically promotes monocyte migration. In an attempt to establish a direct link between VB-201 and MOSPD2 with regards to migration, U937 cells in which MOSPD2 was silenced with sh-RNAs targeting two different regions were tested for transwell migration compared with sh-Control cells in the presence of VB-201. Fig. 5A demonstrates that the level of MOSPD2 silencing varied depending on the sh-RNA used. Specifically, the lower the mRNA (the greater its silencing), the less MOSPD2 protein precipitated with BIO-VB-201 (Fig. 5B). When VB-201 was added to cells treated with sh-Control, migration dropped by 32%. Adding VB-201 to moderately MOSPD2-silenced cells (sh-MOSPD2 #2) further decreased migration by another 43%. However, when MOSPD2 was silenced more profoundly (sh-MOSPD2 #1), VB-201 had no additional effect on cell migration (Fig. 5C).

MOSPD2 regulates primary monocyte migration

Subcellular fractionation of primary $CD14^+$ monocytes and overexpression staining confirmed that MOSPD2 is expressed in the membrane fraction (Fig. 6A, 6B). In an attempt to determine whether MOSPD2 promotes the migration of primary human monocytes, we generated mAbs against human MOSPD2 and

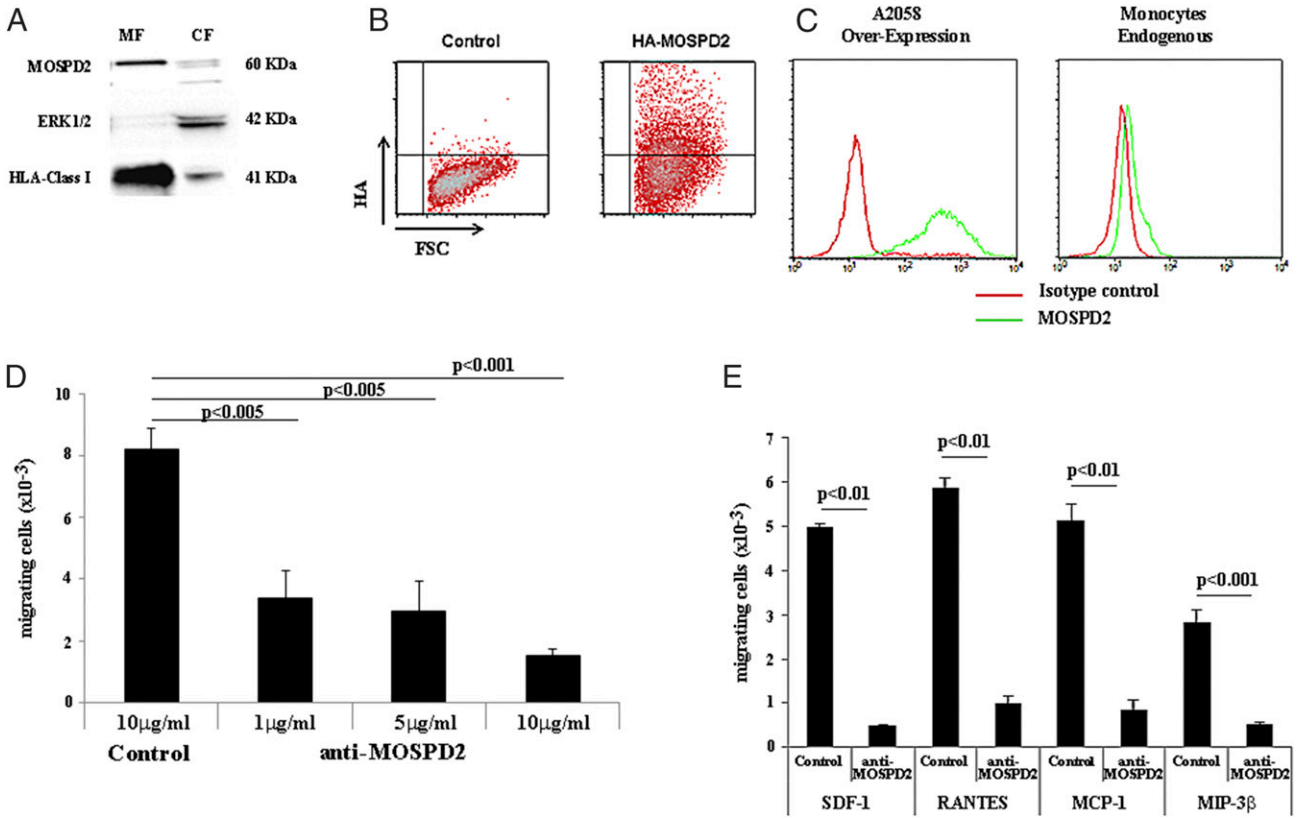

FIGURE 6. MOSPD2 is essential for migration of primary human monocytes. (**A**) Subcellular localization of MOSPD2. Cytoplasmic (CF) and membrane (MF) compartments were fractionated from CD14$^+$ monocytes. One of three experiments is shown. (**B**) HEK 293 cells were transfected with control or HA-tagged MOSPD2-expressing plasmid. Surface staining of cells was performed with anti–HA-PE Ab. One of three experiments is shown. (**C**) A2058 melanoma cells overexpressing HA-tagged MOSPD2 or CD14$^+$ monocytes were stained with 2 μg control human IgG1 Ab or human anti-MOSPD2 mAb for 30 min followed by incubation with Alexa Fluor 647 F(ab′)2 goat anti-human IgG F(ab′)2 for 30 min (1:200). Results for A2058 and monocytes are of gated live and CD14$^+$ cells, respectively. (**D** and **E**) Three-hour transwell migration of freshly isolated human primary monocytes incubated with different concentrations of anti-MOSPD2 mAb compared with 10 μg/ml of control human IgG1 Ab toward 25 ng/ml of SDF-1 (D) or various chemokines (E). Cell count is presented. Samples were run in triplicate. One of three experiments is shown.

tested their effect on migration. Fig. 6C shows staining with one mAb on cells that stably overexpress MOSPD2 and on primary CD14$^+$ monocytes. When tested in a migration assay, anti-MOSPD2 Ab significantly inhibited migration of primary monocytes toward SDF-1 in a dose-dependent manner (Fig. 6D). This inhibition was not restricted to any one chemokine, as similar inhibitory effects were observed with different chemokines (Fig. 6E).

MOSPD2 is abundant in myeloid cells

We next sought to examine whether MOSPD2 abundance and its role in migration are restricted to monocytes. First, MOSPD2 mRNA level was assessed in purified peripheral T and B lymphocytes and neutrophils compared with monocytes. The data presented in Fig. 7A demonstrate that MOSPD2 is predominantly expressed in human monocytes and to a somewhat lesser degree in neutrophils, compared with a near lack of expression in lymphocytes. Next, the role of MOSPD2 in the migration of the immune cell subsets was analyzed. Similar to the previously mentioned results, anti-MOSPD2 mAb profoundly inhibited the migration of monocytes. However, the extent of migration of T cells treated with anti-MOSPD2 Ab was comparable to that of T cells treated with isotype control Ab. In addition, neutrophil migration was reduced by ~40% in the presence of anti-MOSPD2 Ab (Fig. 7B). At steady state, macrophages maintain their numbers within tissues by self-renewal, but tissue assault induces monocyte recruitment and subsequent proliferation of monocyte-derived macrophages in tissues (16, 17). To examine whether MOSPD2 expression is attenuated in macrophages, peripheral blood monocytes were differentiated into M1 proinflammatory or M2 macrophages, which are associated with resolution of inflammation. Fig. 7C demonstrates notable and comparable MOSPD2 expression in M1 and M2 macrophages.

Discussion

Interactions between chemokine receptors and their ligands are promiscuous. This has likely made attempts to therapeutically perturb leukocyte migration by specifically targeting only one chemokine or its counter receptor/s futile. In this study, the functional identification of a protein named MOSPD2 in myeloid cells is presented, to our knowledge, for the first time. Through the observation that VB-201, an oxidized phospholipid, inhibits monocyte migration, precipitation experiments revealed that VB-201 links to MOSPD2 in monocytes. Assessment of MOSPD2 in immune cell subsets showed it is predominantly found in monocytes and neutrophils and to a much lesser degree in lymphocytes, suggesting expression is specific to myeloid cells. Using specific sh-RNA and neutralizing Abs, we discovered that MOSPD2 regulates monocyte and neutrophil migration. Mechanistically, silencing MOSPD2 inhibited signaling events following chemokine receptor ligation, regardless of the activating ligand. In line with its low expression in lymphocytes, MOSPD2 did not play a role in chemokine-induced migration of T cells.

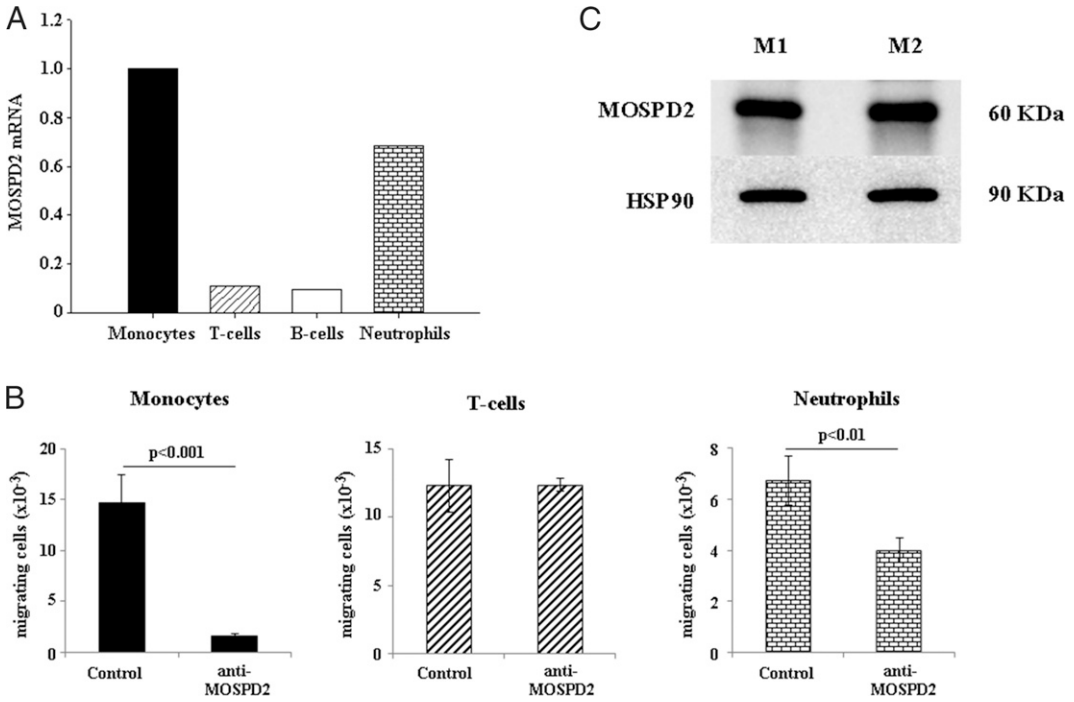

FIGURE 7. MOSPD2 abundance and role in chemotaxis are restricted to myeloid cells. (**A**) mRNA expression of MOSPD2 in purified $CD14^+$ monocytes, B cells, T cells, and neutrophils. 18S was used to normalize RNA levels. Results are shown as expression relative to monocytes. Samples were run in triplicate. One of three to four tested subjects is shown. (**B**) Transwell migration of $CD14^+$ monocytes and T cells toward SDF-1 (100 ng/ml) and of neutrophils toward RANTES (100 ng/ml) in the presence of 10 μg/ml of isotype control or anti-MOSPD2 mAb. Cell count is presented. Samples were run in triplicate. One of three experiments is shown. (**C**) $CD14^+$ monocytes were differentiated with GM-CSF (100 ng/ml) or M-CSF (100 ng/ml) to generate M1 or M2 macrophages, respectively. Samples were blotted to detect the protein level of MOSPD2. HSP90 was used as loading control. One of three experiments is shown.

In experiments designed to determine whether VB-201 activity is specific to MOSPD2, adding VB-201 revealed an additive effect on the migration of partially downregulated MOSPD2 cells only. This may be explained in at least two ways. Unlike in the markedly MOSPD2-silenced cells where the protein is scarce, when MOSPD2 is partially silenced, VB-201 can engage and neutralize remaining copies of MOSPD2 to further affect migration. Alternatively, it is possible that VB-201 does not act via MOSPD2 to inhibit migration. Some support for the latter explanation comes from our studies on neutrophils. Although we showed previously that VB-201 does not inhibit neutrophil migration (12), in this report neutrophils displayed reduced migration in the presence of anti-MOSPD2 Ab. The absence of a mechanism mediating the effect of VB-201 on migration in neutrophils could be one explanation for this observation, although neutrophils expression of other MOSPD2 isoforms that lack a VB-201 binding region could be another. Generating an Ab that blocks binding of VB-201 to MOSPD2 may advance our understanding of the relation between VB-201, MOSPD2, and migration.

The interacting regions within MOSPD2 that are essential for promoting myeloid cell migration are currently unknown. The UniProt database shows that MOSPD2 contains a CRAL-TRIO domain that spans aa 82–239. This domain is recognized in several proteins and is named after two proteins: the CRAL and TRIO. The CRAL region was demonstrated to bind and transport phospholipids (18, 19) and, therefore, we speculate that VB-201 binds to this part of the protein. TRIO is a guanine exchange factor that interacts with small GTPase proteins including Rho, Ras, and Rac. This group of proteins is well recognized as a regulator of cell migration, which insinuates that the TRIO region might mediate the effect of MOSPD2 on cell motility. Elucidating the precise region in MOSPD2 that facilitates its function is of great importance to the further development of inhibitory compounds. Nevertheless, sequence analysis using UniProt predicts that MOSPD2 does not incorporate a cytoplasmic tail, probably preventing the sending of downstream signaling. Alternatively, MOSPD2 may pair with chemokine receptors or other surface membrane proteins to serve as a coreceptor in a complex that is necessary for full activation of chemokine receptors. Experiments to identify potential partners for MOSPD2 are underway.

A line of evidence from animal models is implicating monocytes, and more recently neutrophils, in the pathogenesis of inflammatory diseases and cancer metastasis. We therefore propose MOSPD2 as a potential target for treating diseases in which the accumulation of monocytes and neutrophils is associated with disease progression.

Disclosures

The authors are employees and stock option holders of VBL Therapeutics.

References

1. Griffith, J. W., C. L. Sokol, and A. D. Luster. 2014. Chemokines and chemokine receptors: positioning cells for host defense and immunity. *Annu. Rev. Immunol.* 32: 659–702.
2. Moore, K. J., F. J. Sheedy, and E. A. Fisher. 2013. Macrophages in atherosclerosis: a dynamic balance. *Nat. Rev. Immunol.* 13: 709–721.
3. Soehnlein, O., M. Drechsler, Y. Döring, D. Lievens, H. Hartwig, K. Kemmerich, A. Ortega-Gómez, M. Mandl, S. Vijayan, D. Projahn, et al. 2013. Distinct functions of chemokine receptor axes in the atherogenic mobilization and recruitment of classical monocytes. *EMBO Mol. Med.* 5: 471–481.
4. Boring, L., J. Gosling, M. Cleary, and I. F. Charo. 1998. Decreased lesion formation in $CCR2^{-/-}$ mice reveals a role for chemokines in the initiation of atherosclerosis. *Nature* 394: 894–897.
5. Yamasaki, R., H. Lu, O. Butovsky, N. Ohno, A. M. Rietsch, R. Cialic, P. M. Wu, C. E. Doykan, J. Lin, A. C. Cotleur, et al. 2014. Differential roles of microglia and monocytes in the inflamed central nervous system. *J. Exp. Med.* 211: 1533–1549.
6. Zhao, Q. 2010. Dual targeting of CCR2 and CCR5: therapeutic potential for immunologic and cardiovascular diseases. *J. Leukoc. Biol.* 88: 41–55.

7. Qian, B. Z., J. Li, H. Zhang, T. Kitamura, J. Zhang, L. R. Campion, E. A. Kaiser, L. A. Snyder, and J. W. Pollard. 2011. CCL2 recruits inflammatory monocytes to facilitate breast-tumour metastasis. *Nature* 475: 222–225.
8. Chittezhath, M., M. K. Dhillon, J. Y. Lim, D. Laoui, I. N. Shalova, Y. L. Teo, J. Chen, R. Kamaraj, L. Raman, J. Lum, et al. 2014. Molecular profiling reveals a tumor-promoting phenotype of monocytes and macrophages in human cancer progression. *Immunity* 41: 815–829.
9. Franklin, R. A., W. Liao, A. Sarkar, M. V. Kim, M. R. Bivona, K. Liu, E. G. Pamer, and M. O. Li. 2014. The cellular and molecular origin of tumor-associated macrophages. *Science* 344: 921–925.
10. Zhou, W., S. Q. Ke, Z. Huang, W. Flavahan, X. Fang, J. Paul, L. Wu, A. E. Sloan, R. E. McLendon, X. Li, et al. 2015. Periostin secreted by glioblastoma stem cells recruits M2 tumour-associated macrophages and promotes malignant growth. *Nat. Cell Biol.* 17: 170–182.
11. Sluijter, M., T. C. van der Sluis, P. A. van der Velden, M. Versluis, B. L. West, S. H. van der Burg, and T. van Hall. 2014. Inhibition of CSF-1R supports T-cell mediated melanoma therapy. *PLoS One* 9: e104230.
12. Feige, E., N. Yacov, Y. Salem, I. Levi, I. Mendel, O. Propheta-Meiran, A. Shoham, R. Hait-Darshan, O. Polonsky, J. George, et al. 2013. Inhibition of monocyte chemotaxis by VB-201, a small molecule lecinoxoid, hinders atherosclerosis development in ApoE$^{-/-}$ mice. *Atherosclerosis* 229: 430–439.
13. Mendel, I., E. Feige, N. Yacov, Y. Salem, I. Levi, O. Propheta-Meiran, A. Shoham, E. Ishai, J. George, D. Harats, and E. Breitbart. 2014. VB-201, an oxidized phospholipid small molecule, inhibits CD14- and Toll-like receptor-2-dependent innate cell activation and constrains atherosclerosis. *Clin. Exp. Immunol.* 175: 126–137.
14. Wain, J. H., J. A. Kirby, and S. Ali. 2002. Leucocyte chemotaxis: examination of mitogen-activated protein kinase and phosphoinositide 3-kinase activation by monocyte chemoattractant proteins-1, -2, -3 and -4. *Clin. Exp. Immunol.* 127: 436–444.
15. Di Lorenzo, A., C. Fernández-Hernando, G. Cirino, and W. C. Sessa. 2009. Akt1 is critical for acute inflammation and histamine-mediated vascular leakage. *Proc. Natl. Acad. Sci. USA* 106: 14552–14557.
16. Epelman, S., K. J. Lavine, and G. J. Randolph. 2014. Origin and functions of tissue macrophages. *Immunity* 41: 21–35.
17. Maridonneau-Parini, I. 2014. Control of macrophage 3D migration: a therapeutic challenge to limit tissue infiltration. *Immunol. Rev.* 262: 216–231.
18. Panagabko, C., S. Morley, M. Hernandez, P. Cassolato, H. Gordon, R. Parsons, D. Manor, and J. Atkinson. 2003. Ligand specificity in the CRAL-TRIO protein family. *Biochemistry* 42: 6467–6474.
19. Saito, K., L. Tautz, and T. Mustelin. 2007. The lipid-binding SEC14 domain. *Biochim. Biophys. Acta* 1771: 719–726.